

Orange Luminescence and Structural Properties of Three Isostructural Halocyclohexylisonitrilegold(I) Complexes

Rochelle L. White-Morris, Marilyn M. Olmstead, and Alan L. Balch*

Department of Chemistry, University of California, Davis, California 95616

O. Elbjeirami and Mohammad A. Omary*

Department of Chemistry, University of North Texas, Denton, Texas 76203

Received February 20, 2003

The preparation of three isonitrile complexes (CyNC)Au^ICl, (CyNC)Au^IBr, and (CyNC)Au^II, along with their structural and spectral characterization, are reported. X-ray crystal structures reveal that these crystallize in the same space group and have closely related structures. The structures involve pleated chains of linear, two-coordinate monomers that are arranged in a head–tail fashion. However, these chains vary significantly in the degree of aurophilic interactions among the individual molecules. Thus, (CyNC)Au^ICl forms infinite chains with alternating Au···Au distances of 3.3894(7) and 3.5816(7) Å. Within the chains of (CyNC)Au^IBr, however, the alternation of Au···Au distances is more pronounced so that there are dimers, with an Au···Au distance of 3.4864(9) Å, and neighboring gold centers at 3.7036(9) Å. In (CyNC)Au^II, the gold–gold contacts do not lie within the range of significant aurophilic bonding. The closest Au···Au distance is 3.7182(11) Å while every other Au···Au distance is 3.9304(12) Å. The steric factor of the X ligand and dipole–dipole interactions between the antiparallel complexes is much more significant than aurophilic interactions in governing the self-association of the complexes in this series. The colorless crystals of each solid display an orange luminescence band with a strikingly large Stokes' shift (~21 000 cm⁻¹, 2.6 eV). However, considerable care had to be taken to ensure that the crystals used for the study of the luminescence were free of a surface impurity that produced a turquoise-green luminescence in (CyNC)Au^ICl. The diffuse reflectance spectra for the solids show a similar three-band pattern in the 200–330 nm range.

Introduction

Although the majority of two-coordinate gold(I) complexes are colorless, many are luminescent in the visible region.¹ The luminescence from such gold(I) complexes has attracted considerable attention because of the variety of factors that can influence the luminescence and the range of novel optical phenomena that have been observed, particularly for crystalline solids. For example, the binuclear dithiocarbamate complex, Au^I₂{S₂CN(*n*-pentyl)₂}₂, studied by Eisenberg, Gysling, and co-workers crystallizes in either colorless or orange forms.² The colorless form is transformed into the

orange, luminescent form ($\lambda_{\text{max}} = 631 \text{ nm}$) when exposed to vapors of organic solvents. The trimer, {Au₃(MeN=COMe)₃}, displays solvoluminescence emission at $\lambda_{\text{max}} = 552 \text{ nm}$ that is triggered by contact of previously photoirradiated crystals with solvents.^{3,4} Crystalline [(CyNC)₂Au^I](PF₆) forms yellow and colorless polymorphs that display distinct luminescence, $\lambda_{\text{max}} = 424 \text{ nm}$ (colorless) or 480 nm (yellow), at 298 K.⁵ Fackler and co-workers showed that colorless crystals of [(1,3,5-triaza-7-phosphaadamantane)₂Au]-[Au(CN)₂] are nonluminescent but become photoluminescent after grinding.⁶ In these examples, the observation of

* Authors to whom correspondence should be addressed. E-mail: omary@unt.edu (M.A.O.); albalch@ucdavis.edu (A.L.B.).

(1) For reviews, see: (a) Forward, J. M.; Fackler, J. P., Jr.; Assefa, Z. In *Optoelectronic Properties of Inorganic Compounds*; Roundhill, D. M., Fackler, J. P., Jr., Eds.; Plenum Press: New York, 1999; p 195. (b) Yam, V. W. W.; Lo, K. K. W. *Chem. Soc. Rev.* **1999**, 28, 323.
(2) Mansour, M. A.; Connick, W. B.; Lachicotte, R. J.; Gysling, H. J.; Eisenberg, R. *J. Am. Chem. Soc.* **1998**, 120, 1329.

(3) Vickery, J. C.; Olmstead, M. M.; Fung, E. Y.; Balch, A. L. *Angew. Chem., Int. Ed. Engl.* **1997**, 36, 1179.

(4) Fung, E. Y.; Olmstead, M. M.; Vickery, J. C.; Balch, A. L. *Coord. Chem. Rev.* **1998**, 171, 151.

(5) White-Morris, R. L.; Olmstead, M. M.; Balch, A. L. *J. Am. Chem. Soc.* **2003**, 125, 1033.

(6) Assefa, Z.; Omary, M. A.; McBurnett, B. G.; Mohamed, A. A.; Patterson, H. H.; Staples, R. J.; Fackler, J. P., Jr. *Inorg. Chem.* **2002**, 41, 6274.

luminescence has been tied to the presence of close Au \cdots Au contacts within the solids. Attractive aurophilic interactions (aurophilic bonding) between closed shell gold(I) centers are generally acknowledged to exist in solids whenever adjacent Au \cdots Au contacts are less than ca. 3.6 Å.^{7,8} Such interactions represent a significant factor in determining the solid-state organization of many gold(I) complexes.^{9,10} Correlation effects strengthened by relativistic effects, as suggested by Pyykkö,^{11,12} and/or hybridization of the 6s and 6p orbitals with the 5d orbitals, as suggested by Hoffmann,¹³ are responsible for the aurophilic bonding. Experimental studies that examined the rotational barriers in binuclear Au(I) complexes have shown that the strength of the attractive aurophilic interaction is comparable to hydrogen bonding, ca. 7–11 kcal/mol.^{14,15}

Aggregation via aurophilic bonding can have a profound influence on the emission of gold(I) complexes. For example, Patterson and co-workers have shown that the simple [Au(CN)₂][−] and [Ag(CN)₂][−] ions aggregate under a range of conditions and that the aggregated forms show remarkable variations in their luminescence.^{16–18} Thus, samples of KCl doped with varying amounts of K[Au(CN)₂] show multiple emissions whose relative intensities depend on the dopant level, temperature, and excitation wavelength.¹⁹ Similarly, the luminescence from solutions of K[Au(CN)₂] can be “tuned” to occur from 275 to 470 nm depending upon the concentration and solvent.²⁰ Related studies have shown that the colorless gold carbene cation [Au{C(NHMe)₂}₂]⁺ aggregates in different fashions in salts with different anions (e.g., (PF₆)[−], (BF₄)[−], Cl[−], Br[−]) and that each salt shows its own unique luminescence.^{21,22}

The neutral isonitrile compounds, (RNC)Au^IX, present a diverse array of supramolecular structures. Variation of the R group produces aggregates that include dimers, one-dimensional extended-chain polymers, and two-dimensional polymeric sheets.^{23–31} Despite the simplicity in their molecular structure, spectroscopic investigations of the (RNC)-Au^IX family of compounds are very limited.^{23,29} However, a photophysical/photochemical study of the closely related (OC)Au^ICl showed that it is luminescent with emission at 663 nm from the solid, while the absorption in solution occurs at ca. 250 nm.³²

A meaningful comparison of intermolecular d¹⁰–d¹⁰ interactions is facilitated through examination of structurally and compositionally similar complexes that crystallize in an isostructural fashion.³³ Thus, by studying isostructural Au(I) and Ag(I) compounds, Schmidbaur and co-workers demonstrated that gold is smaller than silver, contrary to what was believed prior to these studies.³⁴ In another recent comparative study of three complexes that crystallize in the same space group, Fackler and co-workers have shown that the intramolecular Ag–Au bonding in a binuclear organosulfur complex was stronger than the Au–Au and Ag–Ag bonding in the corresponding homonuclear complexes.³⁵

Here, we report the structural and spectral characterization of three newly prepared isonitrile complexes (CyNC)Au^ICl, (CyNC)Au^IBr, and (CyNC)Au^II in order to examine the effects of the different halide ligands on the self-association and the luminescence. A complementary study of a series of complexes of the type (RNC)Au^ICN in which the R group is varied while keeping X = CN has been reported elsewhere.³⁶

Results

Colorless crystals of (CyNC)Au^ICl and (CyNC)Au^IBr were obtained by treating aqueous solutions of HAuCl₄·H₂O or HAuBr₄·H₂O with cyclohexyl isonitrile, which acts both as

- (7) Schmidbaur, H. *Gold: Progress in Chemistry, Biochemistry and Technology*; Wiley: New York, 1999.
- (8) Grohmann, A.; Schmidbaur, H. In *Comprehensive Organometallic Chemistry II*; Abel, E. W., Stone, F. G. A., Wilkinson, G., Eds.; Elsevier: Oxford, 1995; Vol. 3, p 1.
- (9) Jones, P. G. *Gold Bull.* **1986**, *19*, 46; **1983**, *16*, 114; **1981**, *14*, 159; **1981**, *14*, 102.
- (10) Pathaneni, S. S.; Desiraju, G. R. *J. Chem. Soc., Dalton Trans.* **1993**, 319.
- (11) (a) Pyykkö, P.; Li, J.; Runeberg, N. *Chem. Phys. Lett.* **1994**, *218*, 133. (b) Pyykkö, P.; Mendizabal, F. *Chem.–Eur. J.* **1997**, *3*, 1458. (c) Pyykkö, P.; Runeberg, N.; Mendizabal, F. *Chem.–Eur. J.* **1997**, *3*, 1451.
- (12) For a review see: Pyykkö, P. *Chem. Rev.* **1997**, *97*, 597.
- (13) (a) Merz, K. M., Jr.; Hoffmann, R. *Inorg. Chem.* **1988**, *27*, 2120. (b) Jiang, Y.; Alvarez, S.; Hoffmann, R. *Inorg. Chem.* **1985**, *24*, 749. (c) Mehrotra, P. K.; Hoffmann, R. *Inorg. Chem.* **1978**, *17*, 2187. (d) Dedieu, A.; Hoffmann, R. *J. Am. Chem. Soc.* **1978**, *100*, 2074.
- (14) Schmidbaur, H.; Graf, W.; Müller, G. *Angew. Chem., Int. Ed.* **1988**, *27*, 417.
- (15) Harwell, D. E.; Mortimer, M. D.; Knobler, C. B.; Anet, F. A. L.; Hawthorne, M. F. *J. Am. Chem. Soc.* **1996**, *118*, 2679.
- (16) Rawashdeh-Omary, M. A.; Omary, M. A.; Patterson, H. H. *J. Am. Chem. Soc.* **2000**, *122*, 10371.
- (17) Rawashdeh-Omary, M. A.; Omary, M. A.; Shankle, G. E.; Patterson, H. H. *J. Phys. Chem. B* **2000**, *104*, 6143.
- (18) Omary, M. A.; Patterson, H. H. *J. Am. Chem. Soc.* **1998**, *120*, 7696.
- (19) Hettiarachchi, A. R.; Rawashdeh-Omary, M. A.; Kanan, S. M.; Omary, M. A.; Patterson, H. H.; Tripp, C. P. *J. Phys. Chem. B* **2002**, *106*, 10058.
- (20) Rawashdeh-Omary, M. A.; Omary, M. A.; Patterson, H. H.; Fackler, J. P., Jr. *J. Am. Chem. Soc.* **2001**, *123*, 11237.
- (21) White-Morris, R. L.; Olmstead, M. M.; Jiang, F.; Tinti, D. S.; Balch, A. L. *J. Am. Chem. Soc.* **2002**, *124*, 2327.
- (22) White-Morris, R. L.; Olmstead, M. M.; Jiang, F.; Balch, A. L. *Inorg. Chem.* **2002**, *41*, 2313.

- (23) Ecken, H.; Olmstead, M. M.; Noll, B. C.; Attar, S.; Schlyer, B.; Balch, A. L. *J. Chem. Soc., Dalton Trans.* **1998**, 3715.
- (24) Schneider, W.; Angermaier, K.; Sladek, A.; Schmidbaur, H. *Z. Naturforsch. B* **1996**, *51*, 790.
- (25) Bonati, F.; Minghetti, G. *Gazz. Chim. Ital.* **1973**, *103*, 373.
- (26) Eggleston, D. S.; Chodosh, D. F.; Webb, R. L.; Davis, L. L. *Acta Crystallogr.* **1986**, *C42*, 36.
- (27) Lentz, D.; Willemsen, S. *J. Organomet. Chem.* **2000**, *612*, 96.
- (28) Mathieson, T. J.; Langdon, A. G.; Milestone, N. B.; Nicholson, B. K. *J. Chem. Soc., Dalton Trans.* **1999**, 201.
- (29) Perreault, D.; Drouin, M.; Michel, A.; Harvey, P. D. *Inorg. Chem.* **1991**, *30*, 2.
- (30) Liao, R.-Y.; Mathieson, T.; Schier, A.; Berger, R. J.; Runeberg, N.; Schmidbaur, H. *Z. Naturforsch.* **2002**, *57b*, 881.
- (31) Jia, G.; Puddephatt, R. J.; Vittal, J. J.; Payne, N. C. *Organometallics* **1993**, *12*, 263. (b) Jia, G.; Payne, N. C.; Vittal, J. J.; Puddephatt, R. *J. Organometallics* **1993**, *12*, 4771.
- (32) Vogler, A.; Kunkely, H. *J. Organomet. Chem.* **1997**, *541*, 177.
- (33) We use the term “isostructural” for crystals of different compounds that exist with the same space group, with similar cell dimensions, and similar, but not necessarily identical, molecular geometries and supramolecular organizations.
- (34) (a) Tripathi, U. M.; Bauer, A.; Schmidbaur, H. *J. Chem. Soc., Dalton Trans.* **1997**, 2865. (b) Bayler, A.; Schier, A.; Bowmaker, G. A.; Schmidbaur, H. *J. Am. Chem. Soc.* **1996**, *118*, 7006.
- (35) Rawashdeh-Omary, M. A.; Omary, M. A.; Fackler, J. P., Jr. *Inorg. Chim. Acta* **2002**, *334*, 376.
- (36) White-Morris, R. L.; Stender, M.; Tinti, D. S.; Balch, A. L.; Rios, D.; Attar, S. *Inorg. Chem.* **2003**, *42*, 3237.

Table 1. Crystallographic Data

	(CyNC)Au ^I Cl	(CyNC)Au ^I Br	(CyNC)Au ^I I
empirical formula	C ₇ H ₁₁ AuClN	C ₇ H ₁₁ AuBrN	C ₇ H ₁₁ AuIN
fw	341.58	386.04	433.03
color, habit	colorless, plate	colorless, needle	colorless, plate
cryst syst	monoclinic	monoclinic	monoclinic
space group	<i>P</i> 2 ₁ / <i>n</i>	<i>P</i> 2 ₁ / <i>n</i>	<i>P</i> 2 ₁ / <i>n</i>
<i>a</i> /Å	6.065(2)	6.1467(15)	6.3222(19)
<i>b</i> /Å	21.608(8)	21.598(5)	21.610(5)
<i>c</i> /Å	6.614(2)	6.7740(15)	7.1266(18)
β /deg	96.53(2)	96.756(16)	97.439(7)
<i>V</i> /Å ³	861.2(5)	893.1(4)	965.4(4)
<i>Z</i>	4	4	4
<i>T</i> /K	91(2)	91(2)	91(2)
<i>d</i> /g cm ⁻³	2.635	2.871	2.979
μ /mm ⁻¹	17.318	20.875	18.369
R1 ^a (obsd data)	4.4	3.2	6.8
wR2 ^b	9.8	9.3	17.4

$$^a R1 = \sum ||F_o| - F_c| / \sum F_o; \quad ^b wR2 = [\sum [w(F_o^2 - F_c^2)^2] / \sum [w(F_o^2)^2]]^{1/2}.$$

Table 2. Selected Bond Lengths and Angles

	(CyNC)Au ^I Cl	(CyNC)Au ^I Br	(CyNC)Au ^I I
	Distances, Å		
Au–C	1.961(14)	1.972(7)	1.953(14)
Au–X	2.258(4)	2.3728(8)	2.5319(10)
Au(1)–Au(1)′	3.3879(16)	3.4864(9)	3.7182(11)
Au(1)–Au(1)″	3.5875(16)	3.7036(9)	3.9304(12)
	Angles, deg		
X–Au–C	178.2(4)	178.05(17)	178.5(3)
Au–C–N	178.9(13)	178.8(6)	178.4(11)
Au–Au–Au	142.92(4)	140.81(2)	137.40(3)
	Symmetry Code		
′	– <i>x</i> , 2– <i>y</i> , – <i>z</i>	2– <i>x</i> , – <i>y</i> , 2– <i>z</i>	1– <i>x</i> , – <i>y</i> , 1– <i>z</i>
″	– <i>x</i> , 2– <i>y</i> , 1– <i>z</i>	2– <i>x</i> , – <i>y</i> , 1– <i>z</i>	1– <i>x</i> , – <i>y</i> , 2– <i>z</i>

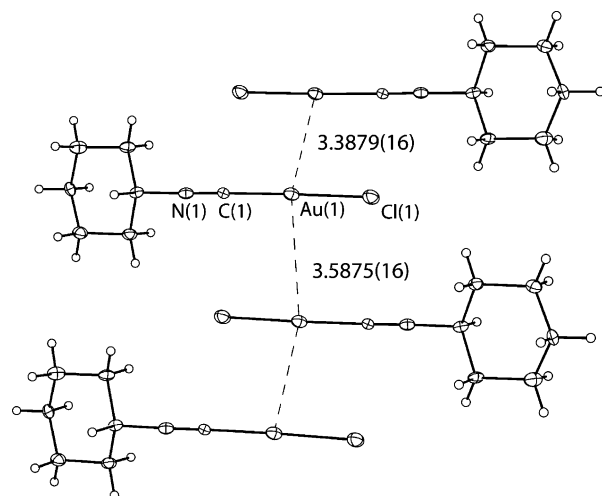
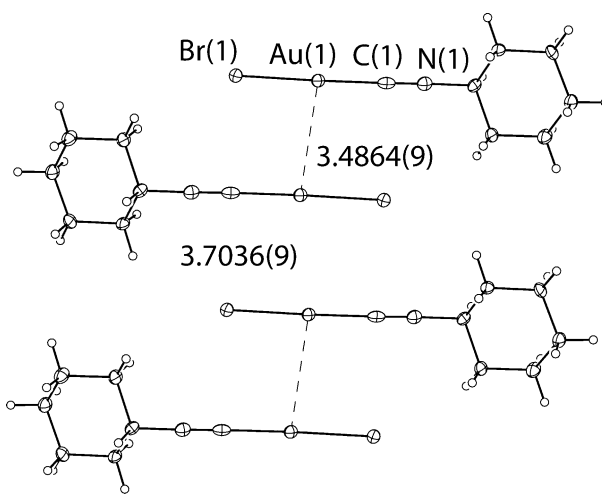
a reducing agent and as a ligand. (CyNC)Au^ICl was also prepared by reaction of (Me₂S)Au^ICl or (tetrahydrothiophene)Au^ICl with cyclohexyl isonitrile. Colorless (CyNC)Au^I was obtained from (CyNC)Au^ICl by metathesis with sodium iodide. Crystallization procedures are given in the Experimental Section.

Crystallographic Studies. The crystal data are given in Table 1. Table 2 contains selected interatomic distances and angles for each of the three neutral complexes. Figures 1, 2, and 3 present diagrams showing the individual molecules and the intermolecular interactions.

Crystals of (CyNC)Au^ICl, (CyNC)Au^IBr, and (CyNC)Au^II are isostructural. The unit cell volume as well as the lengths of the *a* and *c* axes expand in the order Cl < Br < I, as expected from the increasing size of the halide ligand. One molecule is present in each asymmetric unit. Individual molecules in the three compounds differ primarily in the Au–X distances as can be seen from the data in Table 2. Each gold atom is nearly linearly coordinated by the two ligands.

Crystals of (CyNC)Au^ICl grow in two different morphologies, plates, which tend to have rather irregular shapes, and blocks. However, crystallographic data collected on several crystals of both morphologies produced the same structural results.

In (CyNC)Au^ICl, the C–Au distance is 1.961(4) Å and the Au–Cl distance is 2.258(4) Å. For comparison, the C–Au and Au–Cl distances in (*t*-BuNC)Au^ICl are 1.92(1)

**Figure 1.** The structural organization of (CyNC)Au^ICl with 50% thermal contours.**Figure 2.** The structural organization of (CyNC)Au^IBr with 50% thermal contours.

and 2.249(3) Å, respectively.²⁶ In (CyNC)Au^ICl, the cyclohexyl groups are in their normal chair conformations with the isonitrile groups in equatorial positions. Individual molecules of (CyNC)Au^ICl aggregate through aurophilic bonding to form infinite chains with alternating Au···Au distances of 3.3879(16) and 3.5875(16) Å. The chain is pleated with an Au···Au···Au angle of 142.92(4)°.

In the bromo complex, the C–Au and Au–Br distances are 1.972(7) and 2.3728(8) Å while the C–Au–Br angle is 178.05(17)°. These distances are consistent with those in (*t*-BuNC)Au^IBr, where the C–Au and Au–Br distances are 1.939(8) and 2.370(1) Å and the C–Au–Br angle is 177.5(8)°. Molecules of (CyNC)Au^IBr weakly self-associate to form dimers with an Au···Au distance of 3.4864(9) Å. These dimers are situated so that they form extended loose chains with neighboring Au···Au distances of 3.7036(9) Å. While this structure is isostructural with the chloride analogue, the two different aurophilic contacts are roughly 0.10 Å longer in the bromide compound. The Au···Au···Au angle is 140.81(2)°.

In the iodo complex, the C–Au distance is 1.953(14) Å and the Au–I distance is 2.5319(10) Å while the C–Au–I

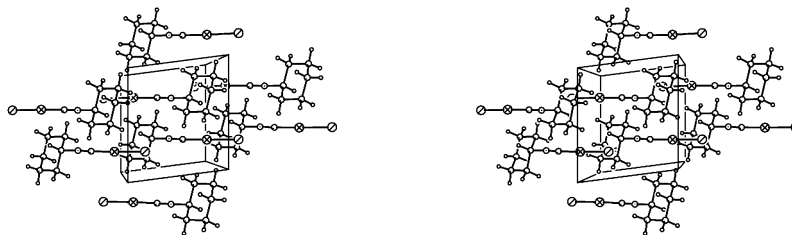


Figure 3. A stereoscopic view of the structure of $(\text{CyNC})\text{Au}^{\text{I}}$. The shortest $\text{Au}\cdots\text{Au}$ contacts are 3.7182(11) and 3.9304(12) Å.

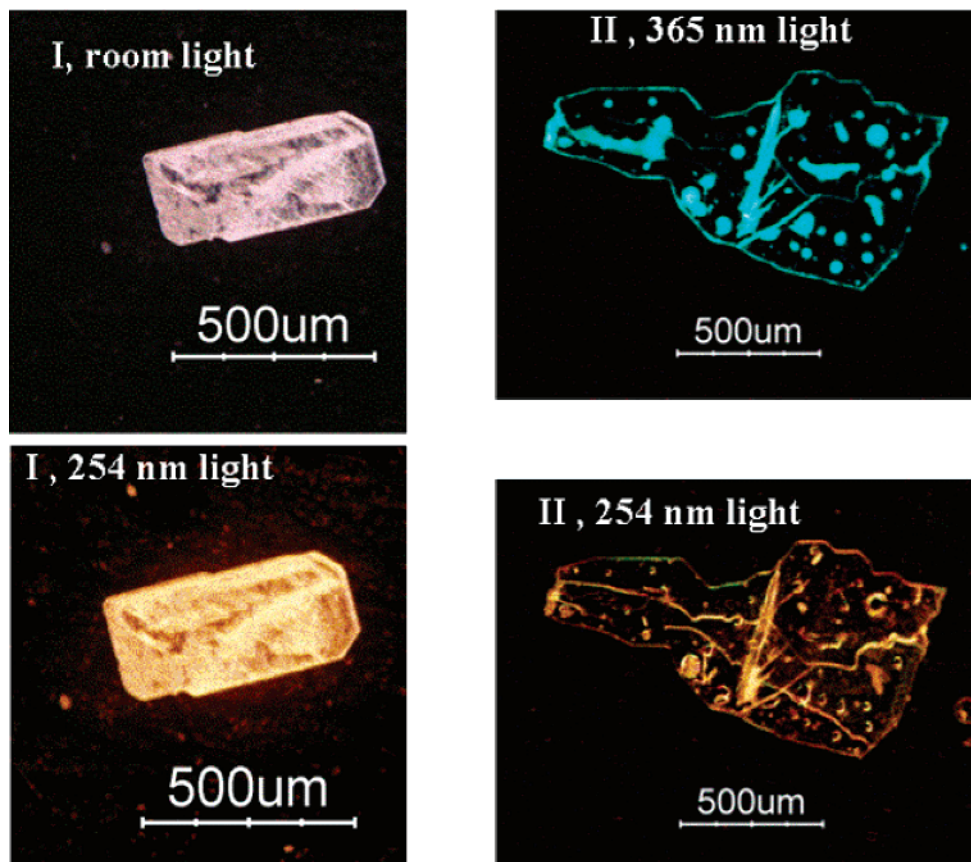


Figure 4. Photographs of the luminescence from two crystals of $(\text{CyNC})\text{Au}^{\text{I}}\text{Cl}$ at ambient temperature. Crystal I (left) shows a uniform orange luminescence upon exciting with 254 nm while crystal II (right) also shows additional turquoise-green luminescence from small portions of the crystal upon exciting with 365 nm. The pictures were taken with a Nikon optical microscope (ECLIPSE ME600L) interfaced with a computer-controlled Nikon digital still camera (DXM12000). Excitations were by means of a hand-held dual-wavelength mercury UV lamp.

angle is $178.5(3)^\circ$. For comparison, the C–Au and Au–I distances in $(t\text{-BuNC})\text{Au}^{\text{I}}$ are 1.95(1) and 2.513(1) Å and the C–Au–I angle is $177(1)^\circ$.³⁰ Although crystals of $(\text{CyNC})\text{Au}^{\text{I}}$ are isostructural with the chloro and bromo analogues, the structure does not contain any gold–gold contacts that are indicative of significant aurophilic bonding. Within the pleated chains of individual $(\text{CyNC})\text{Au}^{\text{I}}$ molecules, the shortest $\text{Au}\cdots\text{Au}$ distance is 3.7182(11) Å and the other $\text{Au}\cdots\text{Au}$ distance is 3.9304(12) Å. The $\text{Au}\cdots\text{Au}\cdots\text{Au}$ angle is $137.40(3)^\circ$.

Spectroscopic Studies. Infrared spectral data for the three complexes are given in the Experimental Section. These spectra are all similar with small differences in the $\nu(\text{CN})$: 2256 cm^{-1} for $(\text{CyNC})\text{Au}^{\text{I}}\text{Cl}$, 2254 cm^{-1} for $(\text{CyNC})\text{Au}^{\text{I}}\text{Br}$,

and 2249 cm^{-1} for $(\text{CyNC})\text{Au}^{\text{I}}$. Since these $\nu(\text{CN})$ values are all larger than that of the free ligand ($\nu(\text{CN}) = 2142\text{ cm}^{-1}$), the isonitrile acts as a strong σ -donor and a weak π -acceptor in this family of complexes.

Crystals of $(\text{CyNC})\text{Au}^{\text{I}}\text{Cl}$, $(\text{CyNC})\text{Au}^{\text{I}}\text{Br}$, and $(\text{CyNC})\text{Au}^{\text{I}}$ display an orange luminescence, the intensity of which is enhanced by lowering the temperature. Figure 4 shows photographs taken under an optical microscope of the luminescence from two crystals of $(\text{CyNC})\text{Au}^{\text{I}}\text{Cl}$ at ambient temperature. Crystal I, which is a block, shows the uniform orange luminescence under irradiation at $\lambda < 280\text{ nm}$. Such luminescence is characteristic of a sample that is pure at the single crystal level. Plates of this material can also show this uniform orange luminescence. Crystal II, which is an

irregular plate, shows a nonuniform luminescence that includes portions with a turquoise-green-emitting material that coats some areas of the crystal. While crystal II was taken from a sample that appears pure, it clearly contains an impurity (as yet unidentified) that is apparent only under microscopic examination with UV light with λ in the range of ca. 320–370 nm. The impurity in crystal II is not discernible under the microscope with the transmitted light. However, with irradiation at $\lambda < 280$ nm, the plate also produces the orange luminescence characteristic of (CyNC)-Au^ICl in all parts of the crystal. Crystals of both types were indistinguishable by single-crystal X-ray diffraction. We have collected X-ray data for several (CyNC)Au^ICl crystals of both types. All of these crystals gave the same structure reported above, and there was no correlation between the presence of the impurity emission with the *R* value. The powder from which both crystals shown in Figure 4 were synthesized shows a uniform turquoise-green emission with a spectrum identical to that for the nonuniform emission of type II crystals ($\lambda_{\text{max}} \sim 485$ nm for both). However, we were unable to grow single crystals that show this uniform turquoise-green emission. Elemental analysis shows no significant difference in the C, H, and N content for the two crystal types and the powder. The three samples gave satisfactory analysis for the (CyNC)Au^ICl formula (see the Experimental Section). We have collected powder X-ray diffraction from the uniformly turquoise-green-emitting powder. The resulting powder pattern was different from that of the calculated powder pattern for the single crystals (see Supporting Information). This suggests the presence of another (CyNC)Au^ICl species that is responsible for the turquoise-green emission. While these data do not give the structure of this species, it is likely either a polymorph or a constitutional isomer, [(CyNC)₂Au][AuCl₂]. The experimental data suggest that the two solid forms dissociate to the same molecule in solution. Conventional analysis methods (¹H and ¹³C NMR, IR, melting points, UV–vis), like elemental analysis, did not distinguish the various forms from one another (see the Experimental Section). Among the various experimental techniques that we pursued, only luminescence spectroscopy and powder X-ray diffraction distinguished the two solid forms of (CyNC)Au^ICl. These observations demonstrate the need to be very careful in monitoring the luminescence from solid samples of such complexes and the need to ascertain their homogeneity at the single-crystal level.

Figure 5 shows the luminescence emission and excitation spectra of carefully selected, homogeneously emitting crystals of the three complexes at 77 K. The broad and structureless emission ($\lambda_{\text{max}} \sim 610$ nm for (CyNC)Au^ICl and (CyNC)Au^IBr and 625 nm for (CyNC)Au^II) has a similar profile for the three complexes. Interestingly, rather short-wavelength UV excitation ($\lambda \leq 280$ nm) is required to generate the orange emission in all three complexes. Lifetime measurements using 265-nm laser excitation yielded $\tau = 30$, 47, and 18 μs ($\pm < 1 \mu\text{s}$) for (CyNC)Au^ICl, (CyNC)Au^IBr, and (CyNC)Au^II, respectively.

Diffuse reflectance spectra acquired for crystals of all three

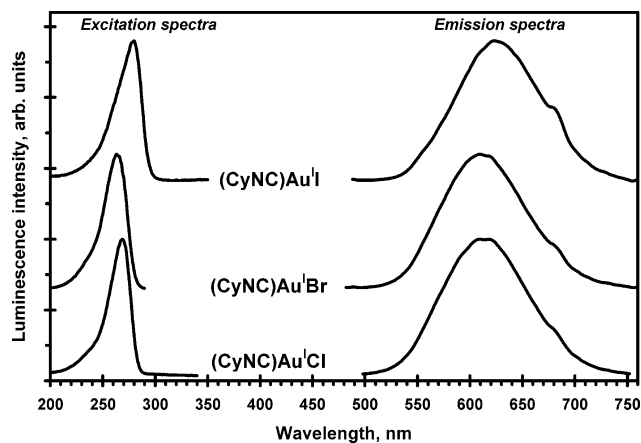


Figure 5. Luminescence emission and excitation spectra for single crystals of (CyNC)Au^ICl, (CyNC)Au^IBr, and (CyNC)Au^II. Excitation at 270 nm was used to generate the emission spectra while the excitation spectra were acquired monitoring the emission maxima.

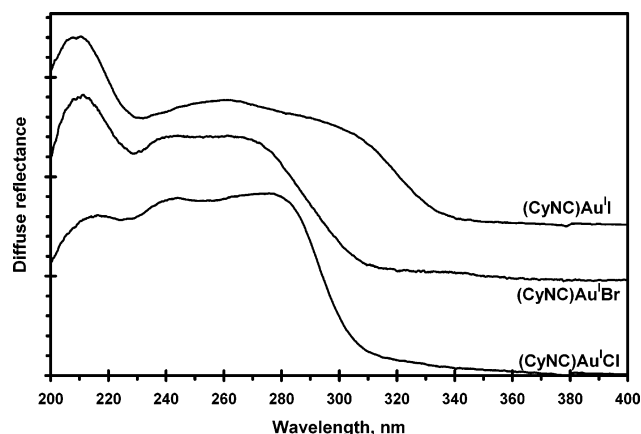


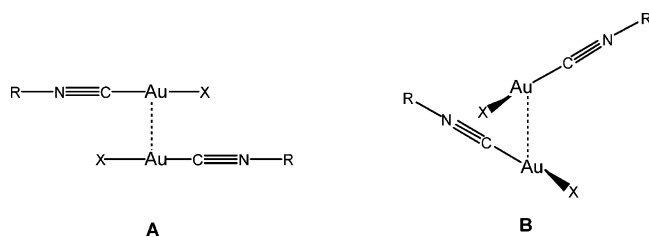
Figure 6. Diffuse reflectance spectra for crystalline samples of (CyNC)Au^ICl, (CyNC)Au^IBr, and (CyNC)Au^II. The samples used were checked first to ensure that they display only the uniform orange luminescence as illustrated in Figure 4 for (CyNC)Au^ICl.

compounds are shown in Figure 6. The spectra are similar, with each complex showing a three-band pattern in the 200–330 nm region.

Discussion

Structural Properties and Auophilic Interactions. The structural data reported here show that the neutral molecules (CyNC)Au^ICl, (CyNC)Au^IBr, and (CyNC)Au^II crystallize in similar ways into extended, pleated chains through varying degrees of auophilic interactions. The molecules are organized in head–tail orientations along the chains. This arrangement is favored by the alternating orientations of adjacent dipoles of the molecules. The shortest Au⁺⋯Au distances (3.3894(7) and 3.5816(7) Å) are seen in (CyNC)Au^ICl. However, it is important to note that these Au⁺⋯Au separations are longer than those observed between the chains of cations in [Au{C(NHMe)₂}₂](PF₆)·0.5(acetone) (3.1882(1) Å)²¹ and in the two polymorphs of [(CyNC)₂Au^I](PF₆) (colorless, 3.1822(3) Å; yellow, 2.9803(6), 2.9790(6), 2.9651(6), and 2.9643(6) Å).⁵ The alternating Au⁺⋯Au separations in (CyNC)Au^IBr are 3.4864(9) and 3.7036(9) Å so that the structure is best considered as containing pairs

Chart 1



of molecules connected by a single auriphilic interaction. In $(\text{CyNC})\text{Au}^{\text{I}}$, the $\text{Au}\cdots\text{Au}$ separations are even larger, 3.7182(11) and 3.9304(12) Å, and are beyond the range where there is significant auriphilic interaction.

Self-association of two-coordinate gold(I) complexes can involve an interaction through the antiparallel orientation shown as **A** in Chart 1 or via the staggered orientation shown as **B** in this chart. A database analysis has shown that shorter contacts are found with the staggered orientation **B**.¹⁰ In the series $(\text{CyNC})\text{Au}^{\text{I}}\text{Cl}$, $(\text{CyNC})\text{Au}^{\text{I}}\text{Br}$, and $(\text{CyNC})\text{Au}^{\text{I}}\text{I}$, all $\text{Au}\cdots\text{Au}$ interactions are of the antiparallel type **A**.

The present study and several others on related complexes offer the opportunity to gain insight into the effects of different anionic ligands on the auriphilic bonding. Theoretical studies by Pyykkö and co-workers predicted an increase in the strength of the auriphilic bonding for the $\text{H}_3\text{PAu}^{\text{I}}\text{X}$ system in the series of anionic ligands (X) with $\text{F} < \text{CH}_3 < \text{H} < \text{Cl} < \text{CN} < \text{Br} < \text{I} < -\text{SCH}_3$.^{11a} This trend has been confirmed for the set of compounds $(\text{Me}_2\text{PhP})\text{Au}^{\text{I}}\text{X}$ (X = Cl, Br, I) where the $\text{Au}\cdots\text{Au}$ distances shorten as one goes from the chloride complex (3.230(2) Å) to the bromide complex (3.119(2) Å) and to the iodide complex (3.104(2) Å).³⁷ A similar trend has been seen for the pair of complexes (1,3,5-triaza-7-phosphaadamantane) $\text{Au}^{\text{I}}\text{X}$ (X = Cl, Br).³⁸

At first sight, it appears puzzling that the trend in $\text{Au}\cdots\text{Au}$ distances observed here (with $\text{Au}\cdots\text{Au}$ distances in the order: $\text{Cl} < \text{Br} < \text{I}$) is the reverse of the trend observed for the analogous complexes with phosphine ligands. However, compounds in the isonitrile series have the antiparallel arrangement **A** in Scheme 1 while compounds in the phosphine series have the staggered arrangement **B**. Consequently, different contributions from auriphilic interactions and dipolar forces are present in the two different series of complexes. A similar conclusion has been made recently by Schmidbaur, Runeberg, and co-workers based on theoretical predictions for the two series $\text{H}_3\text{PAu}^{\text{I}}\text{X}$ and $(\text{MeNC})\text{Au}^{\text{I}}\text{X}$ with orientations **A** and **B** for each.³⁰ The experimental results for the three isostructural complexes herein support the theoretically predicted trend of $\text{Au}\cdots\text{Au}$ distances for $[(\text{MeNC})\text{Au}^{\text{I}}\text{Cl}]_2$ and $[(\text{MeNC})\text{Au}^{\text{I}}\text{I}]_2$ model dimers with the antiparallel geometry (**A**), for which the calculations predicted $\text{Au}\cdots\text{Au}$ distances of 3.442 and 3.792 Å, respectively.³⁰ Our experimental data verify these theoretical

predictions with excellent agreement, which is amazing given the difference in the R group (Me vs Cy) and packing effects (dimer vs polymer). We conclude that a discussion of the self-association of Au(I) compounds should not be limited to auriphilic bonding as other relevant intermolecular interactions (e.g., dipolar interactions, H-bonding) must be considered as well.

In regard to complexes of the $(\text{RNC})\text{Au}^{\text{I}}\text{X}$ class (with X = Cl, Br, and I), there are now crystallographic data for five series: $(\text{CyNC})\text{Au}^{\text{I}}\text{X}$ (this work), $(t\text{-BuNC})\text{Au}^{\text{I}}\text{X}$,^{24,26,30} $(\text{MeOC}(\text{O})\text{CH}_2\text{NC})\text{Au}^{\text{I}}\text{X}$,²⁴ $(\text{PhNC})\text{Au}^{\text{I}}\text{X}$,²⁴ and $(o\text{-xylylNC})\text{Au}^{\text{I}}\text{X}$.²³ Within these series, variation of the halide does not lead to predictable changes in the relative orientations of adjacent molecules, the mode of self-association, or the $\text{Au}\cdots\text{Au}$ separations. Only with $(\text{CyNC})\text{Au}^{\text{I}}\text{X}$ are all three complexes isostructural. With $(t\text{-BuNC})\text{Au}^{\text{I}}\text{X}$ and $(\text{MeOC}(\text{O})\text{CH}_2\text{NC})\text{Au}^{\text{I}}\text{X}$, the chloride and bromide structures are isostructural and the iodide structure is unique, while for $(\text{PhNC})\text{Au}^{\text{I}}\text{X}$, the bromide and iodide structures are isostructural. With $(o\text{-xylylNC})\text{Au}^{\text{I}}\text{X}$, all three complexes crystallize in different space groups. The compounds $(\text{CyNC})\text{Au}^{\text{I}}\text{X}$ (X = Cl, Br or I), $(\text{MeNC})\text{Au}^{\text{I}}\text{Cl}$, $(t\text{-BuNC})\text{Au}^{\text{I}}\text{X}$ (X = Cl or Br), $(\text{PhNC})\text{Au}^{\text{I}}\text{Br}$, and $(\text{PhNC})\text{Au}^{\text{I}}\text{I}$ all crystallize with the molecules arranged into zigzag chains with antiparallel orientations of individual molecules. The distances between gold centers in these chains generally fall in the range of 3.5–3.7 Å, and the auriphilic bonding interactions within these chains are weak. In this group, $(\text{CyNC})\text{Au}^{\text{I}}\text{Cl}$ has the shortest contact, 3.3894(7) Å.

Optical and Photophysical Properties. The similarity in the absorption, emission, and excitation spectra seen for this series of isostructural complexes suggests that differences in supramolecular organization found in the crystals do not strongly influence the spectroscopy. Thus, the small variations seen in the diffuse reflectance spectra shown in Figure 6 for $(\text{CyNC})\text{Au}^{\text{I}}\text{Cl}$, $(\text{CyNC})\text{Au}^{\text{I}}\text{Br}$, and $(\text{CyNC})\text{Au}^{\text{I}}\text{I}$ are consistent with the relatively small differences in the molecular structure introduced by the differing halide groups. A previous study of the related complex, $(\text{MeNC})\text{Au}^{\text{I}}\text{CN}$, assigned absorptions in the 200–260 nm region to metal–ligand charge transfer (MLCT) transitions.³⁹ A similar assignment of the absorption bands seen in Figure 5 is suggested for the complexes studied here.

All of the complexes examined here show a strikingly large Stokes' shift ($\sim 21\,000\text{ cm}^{-1}$ or $\sim 2.6\text{ eV}$). A Stokes' shift with such a large magnitude indicates that the excited state is rather distorted with different bonding properties from those for the ground state.⁴⁰ The lifetime data, which fall in the range of 20–50 μs , suggest that the orange emission occurs from a triplet excited state, as is common in luminescent Au(I) compounds.¹

Several explanations of the large Stokes' shift present themselves. One possibility involves exciplex formation with

(37) (a) Toronto, D. V.; Weissbart, B.; Tinti, D. S.; Balch, A. L. *Inorg. Chem.* **1996**, *35*, 2484. (b) Weissbart, B.; Toronto, D. V.; Balch, A. L.; Tinti, D. S. *Inorg. Chem.* **1996**, *35*, 2490.

(38) Assefa, Z.; McBurnett, B. G.; Staples, R. J.; Fackler, J. P., Jr.; Assmann, B.; Angermaier, K.; Schmidbaur, H. *Inorg. Chem.* **1995**, *34*, 75.

(39) Chastain, S. K.; Mason, W. R. *Inorg. Chem.* **1982**, *21*, 3717.

(40) (a) Omary, M. A.; Patterson, H. H. In *Encyclopedia of Spectroscopy & Spectrometry*; Academic Press: London, U.K., 2000, pp 1186–1207. (b) Lakowicz, J. R. *Principles of Fluorescence Spectroscopy*; Plenum Press: New York, 1983.

shortening of the Au...Au distances in the excited states. Exciplex formation has been shown to occur for a number of solids containing [Au(CN)₂]⁻ and [Ag(CN)₂]⁻ complexes.^{16–20} Although there is a considerable variation in the Au...Au distances within the series of complexes studied here, these are ground-state distances while distances in the luminescent excited states could be similar for the three complexes. One should realize that short ground-state distances are not required for the observation of exciplex emissions, as is well documented for organic exciplexes.⁴¹ Thus, the fact that the iodo complex, for example, does not exhibit significant ground-state auriphilic bonding does not preclude an exciplex emission. Alternatively, the large Stokes' shift could originate from a geometric distortion of the Au–C–N–C unit, which is a consistent feature in each of the three molecules examined here. Such a distortion could involve a localized range of bond length and bond angle changes within the Au–C–N–C unit that result in a significant change in the excited-state molecular structure without displacement of the bulky cyclohexyl groups or major alteration of the Au...Au interactions. Since the absorption features are consistent with an MLCT process involving the Au–CN unit, alteration of just this portion of the individual molecules is a reasonable consequence of this absorption process. To judge which of these possibilities is more likely, rigorous *ab initio* and density functional theory calculations using configuration interaction methods are being pursued to calculate the optical spectra corresponding to transitions involving each of the aforementioned possible excited states.

The spectroscopic data seen for the series (CyNC)Au^ICl, (CyNC)Au^IBr, and (CyNC)Au^II contrast with recent observations on complexes of type (RNC)Au^ICN.³⁶ In the latter, variation of the alkyl groups produces solids with a range of different patterns of self-association including simple chains, side-by-side chains in which two strands make Au...Au contacts with each other, and two-dimensional sheets. Each of these solids have distinctive absorption bands at longer wavelengths than the molecular MLCT bands and unique luminescence spectra with emission maxima that vary from 371 to 430 nm. Moreover, the excitation maxima also vary over the range of 293–353 nm. Consequently, it was concluded that the spectroscopic features of the series are a consequence of the supramolecular organization of molecules within the solids and that the auriphilic interactions between molecules were crucial for the spectroscopic absorption and emission. The facts that the (CyNC)Au^IX compounds reported here exhibit a different mode of self-association and that the electronic structure is different for halides from that

for cyanide make it hardly surprising to see a different luminescence behavior for the two classes of compounds. However, a further comparison of the properties of (CyNC)Au^ICN and (CyNC)Au^ICl is warranted. Although these two complexes are not isostructural ((CyNC)Au^ICN crystallizes in the monoclinic space group *P*2₁/*c*),³⁶ they both form pleated chains with significant auriphilic bonding. Both structures involve two alternating Au...Au distances: 3.426(3) and 3.442(3) Å in (CyNC)Au^ICN and 3.3879(16) and 3.5875(16) Å in (CyNC)Au^ICl. However, (CyNC)Au^ICN does not show the large Stokes' shift seen for (CyNC)Au^ICl. Rather, (CyNC)Au^ICN exhibits emissions that depend on the excitation wavelength.³⁶ Thus, excitation at 315 nm produces an emission maximum at 403 nm while excitation at 360 nm produces an emission peak at 403 nm along with a shoulder at 460 nm. Clearly, changing from a π -acceptor anionic ligand in (CyNC)Au^ICN to a π -donor anionic ligand in (CyNC)Au^ICl alters the electronic properties of these complexes.

It is interesting to note that the luminescence and absorption characteristics of (CyNC)Au^ICl, (CyNC)Au^IBr, and (CyNC)Au^II are rather similar to those communicated by Vogler and Kunkely for the related compound (OC)Au^ICl, which also exhibits a red-orange luminescence with a large Stokes' shift of ~2.1 eV.³² On the basis of their rather limited data, these authors ascribed the absorption of (OC)Au^ICl to a gold d–s transition and attributed the Stokes' shift to auriphilic interactions between molecules in the excited state. The crystal structure of (OC)Au^ICl shows that the molecules are arranged in a head–tail antiparallel fashion (A in Scheme 1) with a short Au...Au contact of 3.38 Å.⁴² Thus the structure of (OC)Au^ICl resembles that of (CyNC)Au^ICl but with closer Au...Au interactions.

Experimental Section

Materials. Hydrogen tetrachloroaurate monohydrate and hydrogen tetrabromoaurate monohydrate were purchased from Strem Chemicals. Cyclohexyl isonitrile, (Me₂S)AuCl, and sodium iodide were purchased from Aldrich. (THT)AuCl (THT = tetrahydrothiophene) was synthesized by a modification of a published procedure.⁴³ All reactions were carried out under atmospheric conditions unless otherwise indicated.

Synthesis. (CyNC)Au^ICl, Method 1. Tetrachloroauric acid hydrate (340 mg, 1 mmol) was dissolved in 8 mL of water to form a yellow solution. Cyclohexyl isonitrile (400 μ L, 3.2 mmol) was then added to the solution. A yellow solid precipitated immediately. The solution was allowed to stir. Some of the solid dissolved, and a brown solid formed. After 30 min of stirring, the solution was filtered. The aqueous solution was allowed to stand for 2 h while white flakes of a solid formed. The solid was collected by filtration and dried under a vacuum. This solid exhibits a uniform orange luminescence ($\lambda_{\text{max}} \sim 610$ nm). Colorless single crystals of the product were grown by diffusion of *n*-pentane into a dichloromethane solution of the complex at ambient temperature or by cooling a nearly saturated solution of the complex in methanol at 4 °C.

(42) Jones, P. G. *Z. Naturforsch.* **1982**, *37b*, 823.

(43) Usón, R.; Laguna, A. In *Organometallic Syntheses* King, R. B., Eisch, J. J., Eds.; Elsevier: Amsterdam, 1986.

(41) (a) Lowry, T. H.; Schuller-Richardson, K. *Mechanism and Theory in Organic Chemistry*; Harper & Row: New York, 1981; pp 919–925. (b) Turro, N. J. *Modern Molecular Photochemistry*; Benjamin/Cummings: Menlo Park, CA, 1978; pp 135–146. (c) Lamola, A. A. In *Energy Transfer and Organic Photochemistry*; Lamola, A. A., Turro, N. J., Eds.; Wiley-Interscience: New York, 1969; pp 54–60. (d) *The exciplex*; Gordon, M., Ware, W. R., Eds.; Academic Press: New York, 1975. (e) Kopecky, J. *Organic Photochemistry: A Visual Approach*; VCH: New York, 1991; pp 38–40. (f) Michl, J.; Bonacic-Koutecky, V. *Electronic Aspects of Organic Photochemistry*; Wiley: New York, 1990; pp 274–286.

(CyNC)Au^ICl, Method 2. Standard Schlenk-line techniques under nitrogen atmosphere were followed in this method. (THT)AuCl (560 mg, 1.64 mmol) was dissolved in 10 mL of deaerated dichloromethane. Cyclohexyl isonitrile (220 μ L, 1.80 mmol) was then added and the solution was stirred for 2 h, after which the solvent was evaporated under reduced pressure and a white solid formed. The solid was washed several times with pentane, collected by filtration, and vacuum-dried. This method was also followed using (Me₂S)AuCl instead of (THT)AuCl. Thus, reaction of 560 mg (1.90 mmol) of (Me₂S)AuCl with an equimolar or excess amount of cyclohexyl isonitrile yielded 510 mg of (CyNC)Au^ICl (90% yield). Anal. Calcd for C₇H₁₁NAuCl: C, 24.61; H, 3.25; N, 4.10. Found for this powder (which gives uniform turquoise-green luminescence with $\lambda_{\text{max}} \sim 485$ nm): C, 24.71; H, 2.98; N, 4.30. Found for crystals grown from methanol (type I in Figure 4): C, 24.89; H, 3.22; N, 4.11. Found for crystals grown from CH₂Cl₂/*n*-pentane (type II in Figure 4): C, 24.72; H, 3.46; N, 4.23. In addition to elemental analysis, additional techniques that did not distinguish the two solid forms included the following with the data presented in pairs for the samples emitting uniform (turquoise-green, orange), respectively. Melting points: The solid melted sharply at (127–129, 125–127) °C into a colorless liquid. ¹H NMR data in DMSO: (1.36–2.10, 1.37–2.00) ppm (m, 10H) and (4.22, 4.19) ppm (s, 1H). ¹³C NMR data in DMSO: (22.30, 22.27), (24.36, 24.37), (30.74, 30.75), and (54.42, 54.37) ppm. The isonitrile carbon did not appear, which is common for isonitrile compounds²⁴ due to the absence of hydrogen atoms attached to this carbon.

(CyNC)Au^IBr. Cyclohexyl isonitrile (175 μ L, 1.41 mmol) was added to a dark-red solution obtained by dissolving 329.9 mg (0.6373 mmol) of hydrogen tetrabromoaurate hydrate in 7 mL of water in a 25-mL round-bottom flask. When the solution was stirred, the dark-red color disappeared and the solution eventually became clear and colorless, with a hint of a brown suspension. After 30 min of stirring, the aqueous solution was filtered into a 25-mL round-bottom flask where it was allowed to slowly evaporate. A white crystalline precipitate began to form immediately. The solution was allowed to evaporate for a few days, whereupon more crystals formed. Crystals formed in this fashion were suitable for single-crystal X-ray diffraction. The compound was also synthesized by metathesis of (CyNC)Au^ICl with NaBr following a similar procedure to the one described below for (CyNC)Au^II. Anal. Calcd for C₇H₁₁NAuBr: C, 21.78; H, 2.87; N, 3.63. Found: C, 21.96; H, 2.61; N, 3.54.

(CyNC)Au^II. (CyNC)Au^ICl (44.9 mg, 0.131 mmol) was dissolved in 8 mL of dichloromethane and placed in a 25-mL round-bottom flask. Finely ground sodium iodide (107 mg, 0.714 mmol) was added to the solution to form a suspension. This suspension was stirred for 1.5 h in order to allow the metathesis reaction to take place. The suspension was filtered, and the volume of the filtrate was reduced to 3 mL under a vacuum. Petroleum ether was added to the solution, which produced a small quantity of a white solid. This mixture was allowed to evaporate for 2 h. Colorless plates were formed during this process. Anal. Calcd for C₇H₁₁NAuI: C, 19.42; H, 2.56; N, 3.23. Found: C, 19.11; H, 2.59; N, 3.11.

Infrared Data. (CyNC)Au^ICl: 2933, 2856, 2256, 1448, 1361, 1043, and 889 cm⁻¹. (CyNC)Au^IBr: 2933, 2856, 2254, 1448, 1363, 1043, and 896 cm⁻¹. (CyNC)Au^II: 2933, 2854, 2248, 1444, 1360, 1041, and 889 cm⁻¹.

X-ray Crystallography and Data Collection. The crystals were removed from the glass tubes in which they were grown together with a small amount of mother liquor and immediately coated with

paratone oil on a microscope slide. Suitable crystals were mounted on glass fibers with silicone grease and placed in the cold stream of a Bruker SMART CCD with graphite monochromated Mo K α radiation at 90(2) K. No decay was observed in 50 duplicate frames at the end of each data collection. Crystal data are given in Table 1.

The structures were solved by direct methods and refined using all data (based on F^2) using the software of SHELXTL 5.1. A semiempirical method utilizing equivalents was employed to correct for absorption.⁴⁴ Hydrogen atoms were added geometrically and refined with a riding model.

Physical Measurements. The luminescence and diffuse reflectance measurements were carried out at the University of North Texas for crystalline material carefully examined by optical microscopy. In some cases, we noted that the orange-emitting crystals were coated in part with a thin overlayer of a turquoise-green-emitting, but apparently amorphous, material. Crystals exhibiting such irregularities were rejected for use in our studies. Steady-state luminescence spectra were acquired with a PTI QuantaMaster model QM-4 scanning spectrofluorometer equipped with a 75-Watt xenon lamp, emission and excitation monochromators, excitation correction unit, and a PMT detector. The emission spectra were corrected for the detector wavelength-dependent response while the excitation spectra are presented uncorrected due to the unreliability of correction methods at short wavelengths below 250 nm, at which the samples here absorb and the xenon lamp output is rather low. Lifetime data were acquired using a nitrogen laser interfaced with a tunable dye laser and a frequency doubler, as part of fluorescence and phosphorescence subsystem add-ons to the PTI instrument. The 337.1-nm line of the N₂ laser was used to pump a freshly prepared 1×10^{-3} M solution of the organic continuum laser dye Coumarin-540A in ethanol, the output of which was tuned and frequency doubled to attain the 265-nm excitation used to generate the time-resolved data. Diffuse reflectance spectra for single crystals of the compounds packed in a 0.1-mm supracell quartz cuvette were acquired using a 150-mm integrating sphere interfaced to a Perkin-Elmer Lambda 900 double-beam UV/VIS/NIR spectrophotometer. IR spectra were recorded as pressed KBr pellets on a Matteson Galaxie Series FTIR 3000 spectrometer.

Acknowledgment. We thank the donors of the Petroleum Research Fund, administered by the American Chemical Society, for support of this research to A.L.B. (Grant 37056-AC) and the Robert A. Welch Foundation (Grant B-1542) and the University of North Texas Faculty Research Grant for the funding of this research to M.A.O. The Bruker SMART 1000 diffractometer was funded in part by NSF Instrumentation Grant CHE-9808259. We thank Dr. Oliver Chyan and Mr. Praveen Nalla for assisting with acquiring the photographs in Figure 4 with the optical microscope and Dr. Teresa Golden for collecting the powder X-ray diffraction data in the Supporting Information.

Supporting Information Available: Powder diffraction data for (CyNC)Au^ICl (PDF) and X-ray crystallographic files, in CIF format, for (CyNC)Au^ICl, (CyNC)Au^IBr, and (CyNC)Au^II. This material is available free of charge via the Internet at <http://pubs.acs.org>.

IC0341946

(44) SADABS 2.0, Sheldrick, G. M. based on a method of Blessing, R. H. *Acta Crystallogr., Sect. A* **1995**, *A51*, 33.